Chapter 6
Processing with Ultrashort Laser Pulses

Jürgen Reif

Abstract This chapter reviews the peculiarities of ultrashort laser pulse interaction with materials and the consequences for materials processing. After a short introduction, presenting time scales of typical processes and comparing previous results for femtosecond and nanosecond laser pulses, we start with the fundamentals of laser-material coupling. Then we describe energy dissipation dynamics and direct follow-up processes and finish with a consideration of bulk and surface relaxation and structure formation on a time scale much longer than the pulse duration.

6.1 Introduction and General Considerations

This chapter is devoted to the application of ultrashort laser pulses (100 femtoseconds or less) for materials processing and the peculiarities related to that short interaction time. Generally, laser materials processing can be classified in a series of processes: the laser energy is coupled to the material; there, it is dissipated and, finally, results in a material reaction like photochemistry [1], melting [2], ablation [3], and phase transformation [4]. In addition, there may be interactions outside the target material, like absorption of laser energy in an ablation plume (cf. Chap. 4) with subsequent plasma sputtering [5]. Further, postinteraction phenomena can play a role in processing, like self-organized structure formation [6], diffusion, (re-) crystallization, and annealing [7]. The time scales involved may range from a few femtoseconds to several microseconds or even longer (cf. Chap. 3): the basic light absorption occurs instantaneously during illumination. It starts during the first optical cycles or femtoseconds. Photochemistry can set in instantaneously and last for nanoseconds after the illumination stops. Both ablation and melting start around one picosecond after the onset of energy input and then may go on for a considerably

J. Reif
Brandenburgische Technische Universität (BTU) Cottbus and Cottbus JointLab,
Universitätsstrasse 1, 03046 Cottbus, Germany
e-mail: reif@tu-cottbus.de,www.physik.tu-cottbus.de/physik/xp2

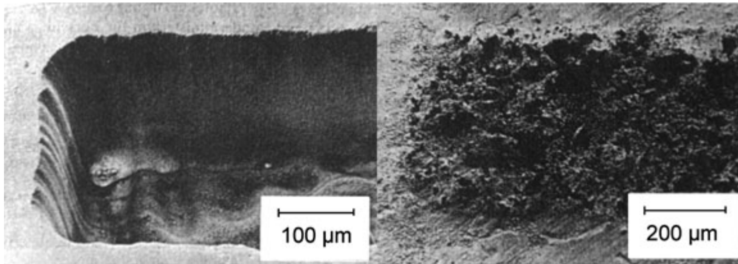

Fig. 6.1 SEM photographs of ablated spots on Teflon for 248-nm-pulses of different duration. *Left panel*: 300 fs (240 pulses at 1 J/cm^2); *Right panel*: 16 ns (50 pulses at 2 J/cm^2) (from [10])

long time. Phase transformation as well as crystallization and annealing may result either from refreezing of the melt or from high ablation-recoil pressure, going on for several microseconds. Usually, laser pulses with a duration of several (ten) nanoseconds are used for materials processing. There, the illumination continues while the material modification already proceeds; i.e., the incident light hits a target with changing (optical) properties. In contrast, pulses of subpicosecond duration open new potentials for laser processing [8]. It becomes possible to concentrate the illumination to only the first steps in the series of processes [9] when a significant material modification has not yet started. Further, the high intensity available at comparably low energy may have implications on both the coupling and the type of materials modification obtainable, as we will show later. Already in the very first reports on materials processing by ultrashort laser pulses [10], a distinct effect was observed: the definition of processed area was, obviously, much cleaner than by processing with nanosecond pulses (cf. Fig. 6.1). This was attributed to the idea that the heat affected zone in the material around the illuminated area was negligibly small, due to an extremely short heat diffusion length during the pulse duration.

To date, it appears, in fact, confirmed that the application of ultrashort laser pulses provides finer, more precise, and better defined results than the use of longer pulses.

6.2 Laser-Material Coupling

As was already addressed in Chap. 3, laser materials processing relies, essentially, on the deposition of light energy into the target, via heating of conduction band electrons or excitation of electrons across the band gap. In principle, band-to-band absorption occurs if the photon energy, $\hbar\omega$, matches the energy gap. Then, the absorbed energy is given by the product of photon energy, $\hbar\omega$, and number, N, of absorbed photons. N is given by the product of absorption probability, $\wp$, and photon density, ρ:

$$W_{\text{abs}} = N\hbar\omega = \wp\rho\hbar\omega. \tag{6.1}$$

For a practical use, it is more convenient to express the absorbed energy in terms of incident fluence, F, i.e., energy area density, and macroscopic absorption cross section, σ:

$$W_{\text{abs}} = \sigma F. \tag{6.2}$$

Classically, σ is a material constant, depending on the absorption strength of the respective transition and on the energy mismatch between photon and material energy structure. All material energy structure depends, however, on *Coulomb* interaction between electrons and atomic cores. Therefore, at very high incident intensity, I, the electric light field

$$E_{\text{light}} = \sqrt{2I/(c\varepsilon_0)} \tag{6.3}$$

may severely perturb the internal *Coulomb* potential and thus influence, transiently, the interaction cross section which is no longer a constant but depends on the laser electric field or rather intensity:

$$\sigma = \sigma(E_{\text{light}}) = \sigma'(I) \tag{6.4}$$

The consequence of this intensity dependent cross section is a nonlinear absorption which will be detailed in the next paragraph.

6.2.1 Nonlinear Absorption

As the electric light field may be considered as a perturbation of the static electronic properties, the nonlinear cross section may be developed in a power series of the incident intensity:

$$\sigma'(I) = \sum_n \sigma^{(n)} I^{n-1}; \quad n = 1, 2, ... \tag{6.5}$$

with $\sigma^{(1)}$ being the "classical," intensity independent, absorption cross section. As a consequence, the absorbed energy becomes:

$$W = \sigma' F = \left(\sum_n \sigma^{(n)} I^{(n-1)}\right) F = \left(\sum_n \sigma^{(n)} I^{(n-1)}\right) I\tau = \sum_n \sigma^{(n)} I^n \tau, \tag{6.6}$$

where τ is the pulse duration[1] and the fluence is $F = I \cdot \tau$. Assuming an incident field $E = E_0 \cdot \exp\{i(\omega t - \mathbf{kr})\}$, the local component ($r = 0$), $E^{(n)} = E^n$, of the perturbing field contains contributions at frequency $n \cdot \omega$, i.e., the interaction energy

[1] For simplicity, here only pulses with rectangular shape in time are considered.

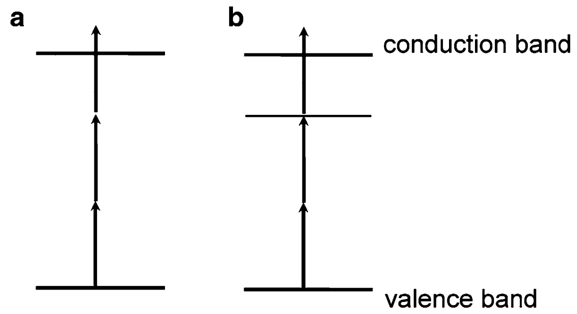

Fig. 6.2 Multiphoton absorption across the band gap. (**a**) Three photon absorption; (**b**) resonance enhancement by defect state

is n times the photon energy. Correspondingly, the interaction may be considered as the simultaneous work of n photons and is termed a "multiphoton" transition. Thus, a nominally "transparent" material can absorb light (Fig. 6.2). The absorption can even be enhanced if there are localized defect states within the band gap.

6.2.2 Hot Electron Generation

If electrons are already present in the conduction band (from multiphoton absorption or intrinsic [metals, semiconductors]), these electrons can be heated by the laser energy and then, potentially, create more hot electrons by avalanche and Auger processes [9,11]. Because of the short pulse duration, the electron heating is much faster than any energy transfer to the lattice, and a "two-temperature" regime is established (high temperature of the electron gas, low lattice temperature) [9, 11]. Target modification, i.e., actual processing, occurs, usually, only after the return to a thermal equilibrium between lattice and electrons which depends on the electron–phonon collision rate.

6.2.3 Incubation

An interesting phenomenon is observed for processing under multiple-pulse irradiation. In particular, in the case of multiphoton absorption, the coupling efficiency increases significantly with successive pulses (Fig. 6.3) In a first attempt to understand this incubation a merely statistical model was introduced [12], assuming the ablation threshold I_t to decrease inversely proportional to a power of the number of pulses N: $I_t(N) \sim 1/N^{\alpha}$. A more "physical" model, assuming an exponential increase of the number of defects (responsible for the threshold reduction), was presented in [13], postulating $I_t(N) \sim \exp(-\alpha N)$. In fact, as is shown in Fig. 6.3, recent experimental results favor this exponential model [14].

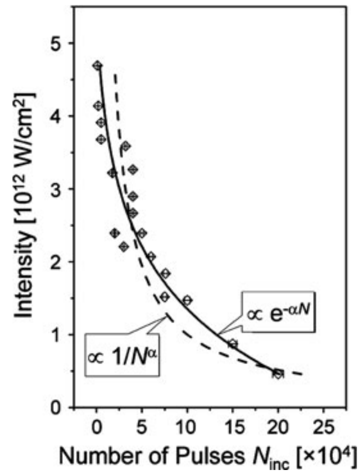

Fig. 6.3 Multipulse (N-on-1) desorption threshold intensity as a function of number N of subsequent pulses [14]. The comparison with the "physical" exponential model (*solid line*) and the statistical model (*dashed line*) confirms the idea of increasing defect generation as the origin of incubation

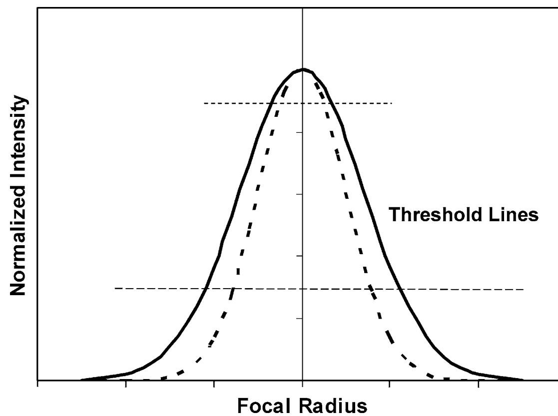

Fig. 6.4 Focal beam profile (*normalized*) for Gaussian beam (*solid line*) and squared Gaussian beam (*dashed line*). The dashed horizontal line indicates the threshold intensity. Obviously, the squared-beam radius is smaller than the diffraction limit, given by the Gaussian beam. The dotted line indicates the situation where only the most intense central part of the beam profile overcomes the action threshold

6.2.4 Resolution Below the Diffraction Limit

Another interesting consequence of multiphoton absorption is the possibility of generating structures below the diffraction limit [15]. This is schematically illustrated in Fig. 6.4 for a two-photon transition: As the absorption cross-section depends, in this case, on the square of the local intensity, the effective spatial beam profile is the square of the original pulse.

Even stronger confinement of the surface interaction region can be obtained by using an optical near-field microscope [16]. Another possibility consists in adjusting the laser pulse peak intensity in the focal region just only slightly above the

threshold for material modification (Sect. 6.5 and Chaps. 3, 5, 7, 8). Then, only the very top of the beam profile will act, thus significantly reducing the modified spot size [17] (cf. dotted line in Fig. 6.4).

6.3 Dissipation Dynamics

Once the laser energy is deposited in the target electronic system, it will be dissipated and transferred to the lattice. Only then, in fact, material modification and processing can take place.

6.3.1 Dissipation Channels

The only direct action of the laser energy input is an ionization of the interaction volume. For further energy dissipation from the electrons to the lattice there are, in principle, two channels: (1) thermodynamic equilibration between electron bath and lattice by electron–phonon collisions [9, 11, 18] and (2) perturbation of crystalline bonds when binding electrons are excited from their state of equilibrium. For channel (2) molecular dynamics calculations [19, 20] and tight-binding simulations [21] indicate that within a few 10 fs the crystalline lattice starts to be severely disturbed and dissolved. The dissolution can go so far that atoms start to leave the crystal surface and, thus, initiate ablation. The subsequent route for channel (1) is more complicated: since the dissipation occurs very rapidly, the temperature can, occasionally, rise accordingly, and homogeneous nucleation may take place in the interaction volume, giving rise to a phase explosion [9, 22, 23]. Usually, the time scale of the actual explosion, i.e., material removal, is at the order of a few nanoseconds. This is significantly *after* the end of energy input. However, the lattice excitation, via both routes (1) and (2), does not necessarily result in ablation. It can, as well, relax via classical thermodynamic pathways into the liquid state and, then, end in (re-)crystallization, again on a time scale much longer than the pulse duration.

6.3.2 Transient Material Modification

As was just indicated, a main feature of materials processing with ultrashort laser pulses is the temporal separation between energy input and (macroscopic) action. This implies that during and immediately after the laser pulse the material is in a transiently modified state. Similar to the effect of incubation, this modified state can result in a changed response to a second laser pulse following immediately after, as shown in Fig. 6.5.

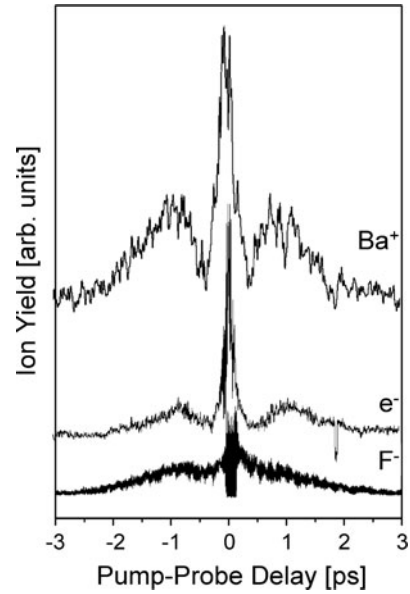

Fig. 6.5 Transient modification of material response: pump-probe investigation of femtosecond laser desorption from BaF_2. For a second pulse about 700 fs after irradiation with a first laser pulse, desorption is significantly enhanced, indicating an increased absorption which, subsequently, decays again

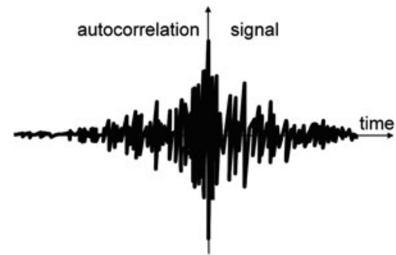

Fig. 6.6 Typical autocorrelation of an "optimally shaped" pulse after phase modulation of a femtosecond pulse in a programmable spatial light modulator (SLM)

This transient modification can be successfully exploited by sending appropriately shaped pulses [24] to the target, which can be considered to produce modulated trains of pulses over a certain range of time (Fig. 6.6). It has been demonstrated [24] that thus the processing result can be optimized.

A particular type of transient material modification is the possibility of driving the target out of thermal equilibrium [6, 25]. Then, classical thermodynamics is no longer a good way of describing the evolution of the system. In fact, pump-probe x-ray diffraction [26–28] indicates the presence of such nonequilibrium systems, also termed "nonclassical liquids," exhibiting the loss of near order but keeping far order. As will be shown later, relaxation from this instability results in a very special type of materials processing, namely self-organized surface structure formation.

6.4 Desorption/Ablation

6.4.1 Concept

One of the most dramatic effects of the laser impact is the removal of material from the target surface. At moderate pulse energy only individual ions or clusters come off, frequently attributed to Coulomb explosion of an electrostatically destabilized surface. However, this "desorption" is, normally, too weak for materials processing. The much stronger removal for this purpose, termed "ablation," occurs only beyond an (empirical) threshold pulse energy. The corresponding processes are more complex than for desorption and combine Coulomb explosion, phase explosion and, potentially, plasma expansion. This plasma is the consequence of an extremely high excitation, with a high density of hot electrons, directly within the target. In contrast to the interaction of longer pulses it does not result from an excitation of the ablation plume in front of the target. Laser ablation is, certainly, the base of the most important field of laser materials processing. Cutting, drilling, lithography but also pulsed-laser-deposition (PLD) rely on this phenomenon. As suggested already by the first experiments [10], the ultra-short-pulse results appear, in most cases, much cleaner and better defined than those obtained with longer pulses [29–42]. Taking into account the timescales and processes involved, the early explanation of a reduced heat affected zone (HAZ) appears evident. Because the energy input is terminated before particle emission occurs, all excited material is ejected, and no additional energy is deposited in the surrounding target region (Fig. 6.7). This has been confirmed experimentally [43].

However, this scenario only holds as long as the initial excitation is not too large. Otherwise, the dissipation rate can be faster than the ablation process, and a larger region than originally irradiated is affected, leading to a heat affected zone similar to the case of long-pulse irradiation.

Once ablated, the material can be recondensed on a substrate in the ablated particle stream. This is the basic idea of pulsed laser deposition of thin films, which is the subject of Chap. 5 of this volume. The peculiarities of using femtosecond laser ablation may be that the ablation plume consists of higher-energetic ions than for longer pulses [44]. On the other hand, the droplet content in the plume is strongly reduced while there is a large amount of ionic clusters [45, 46], resulting in new properties of the deposited films.

6.4.2 Applications

One application of ultrafast (multiphoton-)ablation is, certainly, the direct writing of fine, well-defined structures with a feature size below 1 μm, such as holographic gratings [47] or Fresnel lenses [48] (Fig. 6.8).

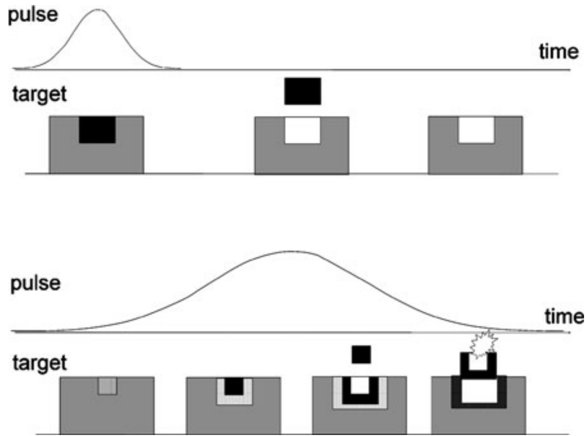

Fig. 6.7 Difference between femtosecond (*upper*) and long-pulse (*lower*) ablation. (The shaded area is the excited region. The darker the shading, the stronger is the excitation). For the short pulse, the irradiated area is immediately highly excited. After a dissipation delay, the whole excited volume is ablated. For the long pulse, at the beginning, only the central part is weakly excited. For increasing pulse duration, the central-part excitation increases above threshold, the surrounding area is weakly excited. Still later (yet during the pulse), the central area material leaves the target, the surrounding reaches the threshold and a still wider range is weakly excited. At the same time, the ablated plume still absorbs laser light, generating a plasma which, for still longer pulse duration, is heated by inverse bremsstrahlung and, then, sputters back to the surface

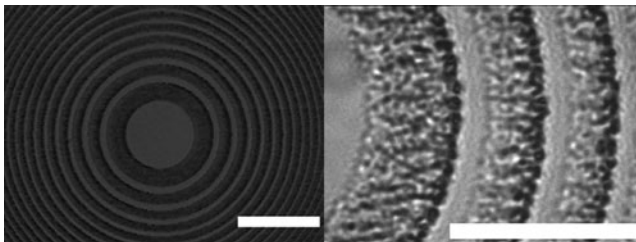

Fig. 6.8 Direct writing of well defined structures with femtosecond laser: Fresnel phase plates infused silica [48], Overview (*left*) and detail (*right*). The white bar corresponds to 100 μm in both panels

Another field is the structuring of thin films on supporting substrates [49]. Of particular interest is the repair of defects in photomasks, e.g., Cr on quartz [40], without affecting the substrate. In another application, tiny pores were introduced in a protective TiN thin film to improve its tribological performance [50] (Fig. 6.9). Again, the low thermal budget of femtosecond processing was necessary to prevent delamination of the thin film.

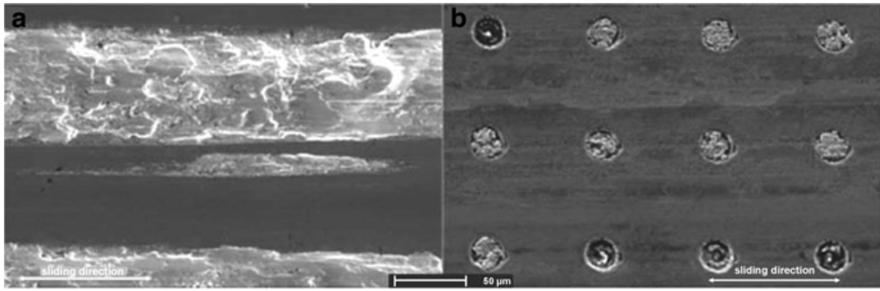

Fig. 6.9 Wear traces on TiN protective film. (*left*: unpatterned; *right*: femtosecond patterned [50])

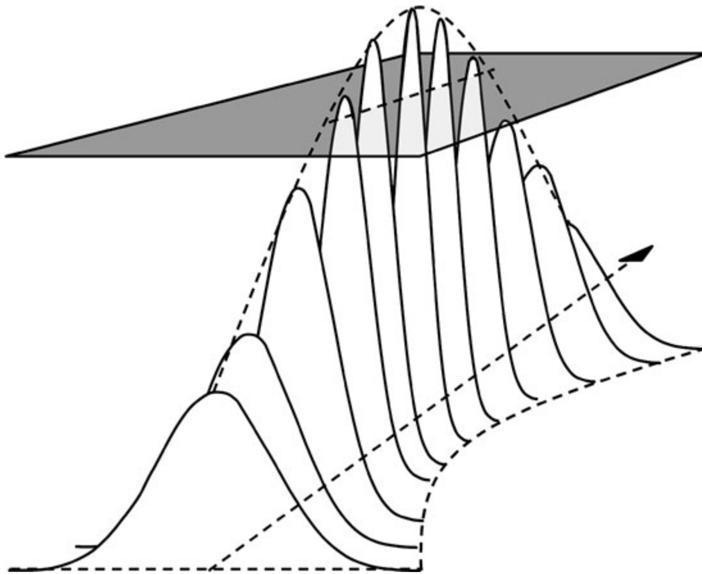

Fig. 6.10 Sketch of the intensity variation in the focal region. The *shaded section* represents the action threshold. It is easily seen, that the threshold intensity is exceeded is only in a limited volume (*unshaded*). Depending on focussing conditions and multiphoton order (cf. Fig. 6.4) this volume can be minimized in 3-D

6.5 3-D Bulk Modifications, Waveguide Writing

Because of the high intensity available at relatively low fluence, the possibility to easily rely on multiphoton absorption with femtosecond pulses opens new channels also for processing in the bulk of a material. Restricting the action volume, where the threshold intensity is exceeded, by tight focussing, even three-dimensional processing becomes feasible (Fig. 6.10).

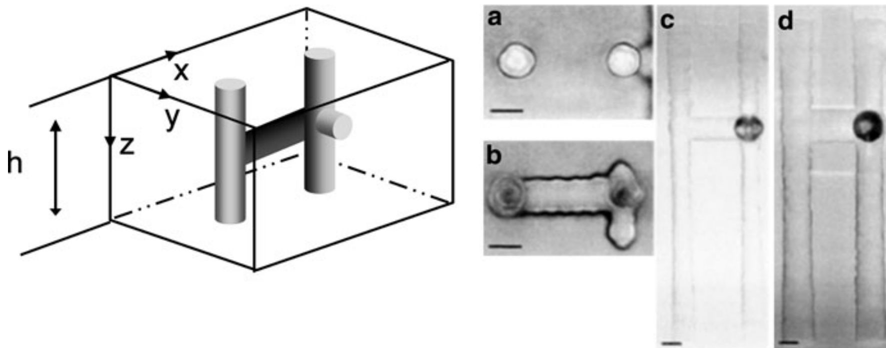

Fig. 6.11 Writing of 3-D structures in fused silica [51]. *Left*: The laser is tightly focused inside the transparent sample. In the focal region, a void is generated after multiphoton absorption and subsequent bond breaking. To write the structure, the sample – and thus the focus – is moved in 3-D. The *right* panel shows the adjacent voids aligned to obtain a trace

6.5.1 Bulk Structuring, Waveguide Writing

This effect is exploited to write structures inside the bulk of a transparent material [51, 52]. The principle is shown in Fig. 6.11.

The laser is focussed into the bulk of the transparent target. Only in the confocal region, the intensity is high enough to allow multiphoton absorption. The resulting ionization, subsequent local plasma formation and lattice destabilization result in a rearrangement of the material, e.g., the generation of voids, on the one hand, and a local densification on the other hand. By moving the focus inside the sample, complex structures can be written [53–56]. An important application of such bulk modification is the writing of micro-channels for lab-on-chip applications [57] and integrated optical waveguides [58–61] and even more complex photonic devices [52].

6.5.2 Multiphoton Polymerization

Even more complicated structures can be produced, not only in the bulk, by exploiting a photochemical reaction, also induced by multiphoton absorption. Light-induced polymerization, usually, requires UV light to induce the reaction. By multiphoton absorption, however, the same transitions in the precursor of the polymer can be used, with the advantage of precise 3-D-localization. Thus, by moving the focal point inside the precursor, complex structures can be polymerized [53, 56, 57, 62–64]. A particularly useful group of materials are photosensitive glasses like, e.g., Ormocer® [65].

6.6 Phase Transformation, Laser Annealing

One of the consequences of the ultrafast perturbation of the target lattice is that the material after relaxation does not return to the phase it was before. Thus, amorphous material can be crystallized if the cooling from the (super-)liquid phase is sufficiently slow [66] (laser annealing). On the other hand, if the cooling is very rapid, an initially crystalline material can turn into the amorphous phase [67]. Both effects have been observed on silicon. The main difference appears to be the surrounding condition: at the surface, crystallization was found, in deep drilled holes the material became amorphous. In any case, the advantage of femtosecond pulses appears to be the very rapid generation of an electron–hole plasma instead of a "regular" liquid as the state of crystal perturbation.

6.7 Medical Applications

An important field of laser materials processing are applications in medicine and biology. The specific point for the application of ultrashort laser pulses lies, again, in the fact that high intensity, enough to enable multiphoton processes, can be obtained at relatively low fluence. Thus, localized action can be achieved without thermally overloading (and potentially destroying) the target. This is particularly important for the isolation and manipulation of single biological cells [68, 69], nanosurgery of cells and tissue [70, 71], or material transfer [72]. But also in more mechanical field, the treatment of dental and bone material, femtosecond lasers are successfully applied [73,74]. Here the advantage lies in the fact that the high intensity achievable makes multiphoton absorption almost as efficient as single photon absorption. Also the interaction is extremely short. Therefore, complex materials, like dental and bone tissue, are ablated simultaneously, independent of their detailed composition.

6.8 Nanostructures and Nanoparticles

As the irradiated target surface is, usually, in a state well away from thermal equilibrium, the emitted material is neither atomized nor does it consist of large droplets from the melt (cf. PLD with femtosecond pulses). If the deposited energy is sufficiently low, so that no hot electron–hole plasma is generated, the ablated material can consist of a mixture of atomic ions, considerably large clusters and even nanoparticles. The latter are, especially, observed, when the ablation takes place under a liquid environment, i.e., the free expansion of the ablation plume

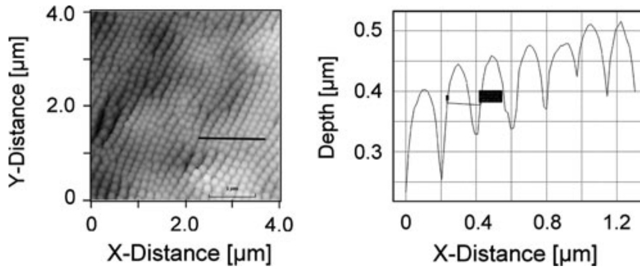

Fig. 6.12 Self-organized regular nanostructure (ripples) upon femtosecond laser ablation with circularly polarized laser light. The *left panel* shows an AFM image of a part of the ablated area, the *right panel* is an analysis along the *black line* in the *right panel*

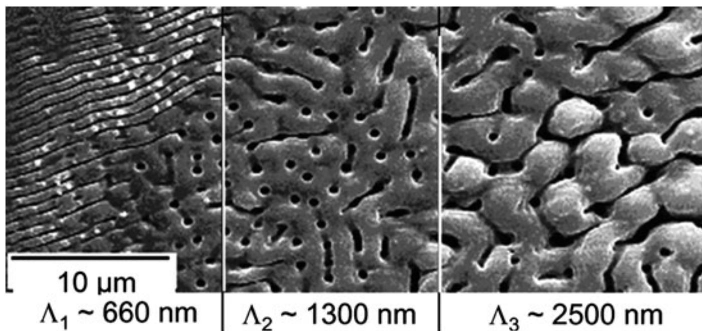

Fig. 6.13 Ripples produced with linearly polarized light on silicon. The image shows a part of the ablated spot, with the spot center at the right and the spot edge to the left. With increasing intensity along the beam profile, the structure becomes coarser, changing in distinct steps of period doubling

is hindered by the surrounding medium [75]. This appears to be a promising way to produce gold colloids which may be used for drug delivery [76, 77]. But even in vacuum, silicon nanoparticles have been produced [78]. Another consequence of the thermodynamic instability, induced in the target upon the rapid energy input, is the phenomenon of self-organized structure formation in the area where ablation took place [6] (Fig. 6.12).

The dynamics of the formation of these structures, called "ripples", is still not fully understood. Their features depend, however on the absorbed energy dose. Typical for self-organization, they exhibit, e.g., phenomena like period doubling under an increase of energy across the beam profile (Fig. 6.13).

It has been shown, recently, that it is possible to produce arrays of ripples structures, coherently covering larger areas [79–81]. Such larger areas can, then, be used as stencils to produce replica showing a maximized hydrophobicity, the so-called "lotus-effect" [82].

6.9 Conclusions

Materials processing using ultrashort laser pulses provide some distinct features of interest, compared to the application of longer pulses. First of all, the energy input is usually separated from the subsequent steps leading to materials modification. Second, the high intensity at comparably low fluence facilitates, on the one hand, multiphoton interaction and reduces, on the other hand, the thermal load on the target. The second point is responsible for the outstanding precision and cleanliness of the processing, the first point accounts for the finesse of possible results, well confined and smaller than the diffraction limit.

Acknowledgements The author gratefully acknowledges fruitful discussions with Markus Ratzke, Florenta Costache, Taznimir Arguirov, Michael Bestehorn, and Olga Varlamova.

References

1. H. Sato, S. Nishio, J. Photochem. Photobiol. C Photochem. Rev. **2**, 139 (2001)
2. L.S. Penn, R. Lin, B.S. Yilbas, Opt. Lasers Eng. **27**, 297 (1997)
3. see, e.g., the proceedings of the *Conferences on Laser Ablation (COLA)*:
   J.C. Miller, R.F. Haglund (eds.), *Laser Ablation: Mechanisms and Applications*, Lecturer Notes in Physics **389**, (Springer, Heidelberg, 1991)
   J.C. Miller, D.B. Geohegan, (eds.), *Laser Ablation: Mechanisms and Applications - II*, AIP Conference Proceedings **288** (American Institute of Physics, New York, 1994)
   E. Fogarassy, D.B. Geohegan, M. Stuke (eds.), *Proceedings of Symposium F: Third International Symposium on Laser Ablation of the 1995 E-MRS Spring Conference*, Appl. Surf. Sci. **96–98**, 1 (1996)
   R.E. Russo, D.B. Geohegan, R.F. Haglund, R.F. Haglund Jr., K. Murakami (eds.), *Proceedings of the 4th Conference on Laser Ablation*, Appl. Surf. Sci. **127–129**, 1 (1998)
   J.S. Horwitz, H.U. Krebs, K. Murakami, M. Stuke (eds.), *Laser Ablation V*, Appl. Phys. A **69**(Supplement 1) (1999)
   K. Murakami, A. Yabe, J.S. Horwitz, C. Fotakis, J.T. Dickinson (eds.), *Proceedings of the 6th Conference on Laser Ablation*, Appl. Surf. Sci. **197–198**, 1 (2002)
   C. Fotakis, H. Koinuma, D. Lowndes, M. Stuke, (eds.), *Laser Ablation VII*, Appl. Phys A **79**(4–6), 713 (2004)
   B. Luk'yanchuk, S. Juodkazis, T. Lippert (eds.), *Special Issue: Laser Ablation Fundamentals*, Appl. Phys. A **92**, 743 (2008)
   P. Schaaf, R. Serna, J.G. Lunney, E. Fogarassy (eds.), *Laser synthesis and processing of advanced Materials*, Appl. Surf. Sci. **254(4)**, 789 (2007)
4. A. Kaplan, Chap. 3 in *The Theory of Laser Materials Processing*, Springer Ser. Mater. Sci ed. by J. Dowden (Springer, 2009), p. 119
5. S. Eliezer, K. Mima (eds.), *Applications of Laser-Plasma Interactions*, Series in Plasma Physics, (CRC, 2009)
6. J. Reif, F. Costache, M. Bestehorn, Chap. 9 in *Recent Advances in Laser Processing of Materials*, ed. by J. Perriere, E. Millon, E. Fogarassy (Elsevier, 2006) p. 275
7. I.W. Boyd, J.I.B. Wilson, Nature **287**, 278 (1980)
8. R.R. Gattass, E. Mazur, Nat. Photonics **2**, 219 (2008)
9. D. von der Linde, K. Sokolowski-Tinten, Appl. Surf. Sci. **154–155**, 1 (2000)
10. S. Küper, M. Stuke, Appl. Phys. Lett. **54**, 4 (1989)

11. B. Rethfeld, K. Sokolowski-Tinten, D. von der Linde, S. Anisimov, Appl. Phys. A **79**, 767–769 (2004)
12. Y. Jee, K. Becker, R.M. Walser, J. Opt. Soc. Am. B **5**, 648 (1988)
13. S. Petzoldt, A.P. Elg, J. Reif, E. Matthias, Proc. SPIE **1438**, 180 (1989)
14. F. Costache, S. Eckert, J. Reif, Appl. Phys. A **92**, 897 (2008)
15. A. Ostendorf, F. Korte, G. Kamlage, U. Klug, J. Koch, J. Serbin, N. Baersch, T. Bauer, B.N. Chichkov, Chap. 12 in *3D Laser Microfabrication: Principles and Applications*, ed. by H. Misawa, S. Joudkazis (Wiley, 2006)
16. S. Nolte, B.N. Chichkov, H. Welling, Y. Shani, K. Lieberman, H. Terkel, Opt. Lett. **24**, 914 (1999)
17. F. Korte, S. Adams, A. Egbert, C. Fallnich, A. Ostendorf, S. Nolte, M. Will, J.-P. Ruske, B.N. Chichkov, A. Tünnermann, Opt. Express **7**, 41 (2000)
18. S.-S. Wellershoff, J. Hohlfeld, J. Güdde, E. Matthias, Appl. Phys. A **69**, S99 (1999)
19. P. Lorazo, L.J. Lewis, M. Meunier, Phys. Rev. Lett. **91**, 225502 (2003)
20. Z. Lin, L.V. Zhigilei, Phys. Rev. B **73**, 184113 (2006)
21. H.O. Jeschke, M.E. Garcia, M. Lenzner, J. Bonse, J. Krüger, W. Kautek, Appl. Surf. Sci. **197–198**, 839 (2002)
22. N. Bulgakova, I.M. Bourakov, Appl. Surf. Sci. **197–198** (2002)
23. R. Kelly, A. Miotello, Phys. Rev. E **60**, 2616 (1999) A. Miotello and R. Kelly, Appl. Phys. Lett. **67**, 3535 (1995) A. Peterlongo, A. Miotello, and R. Kelly, Phys. Rev. E **50**, 4716 (1994)
24. R. Stoian, A. Mermillod-Blondin, S.W. Winkler, A. Rosenfeld, I.V. Hertel, M. Spyridaki, E. Koudoumas, P. Tzanetakis, C. Fotakis, I.M. Burakov, N.M. Bulgakova, Opt. Eng. **44**, 051106 (2005)
25. P. Saeta, J.-K. Wang, Y. Siegal, N. Bloembergen, E. Mazur, Phys. Rev. Lett. **67**, 1023 (1991)
26. A.M. Lindenberg, S. Engemann, K.J. Gaffney, K. Sokolowski-Tinten, J. Larsson, D. Reis, P. Lorazo, J.B. Hastings, SPIE Proc. **7005**, 700504 (2008)
27. A. Lindenberg, S. Engemann, K. Gaffney, K. Sokolowski-Tinten, J. Larsson, P. Hillyard, D. Reis, D. Fritz, J. Arthur, R. Akre, M. George, A. Deb, P. Bucksbaum, J. Hajdu, D. Meyer, M. Nicoul, C. Blome, Th. Tschentscher, A. Cavalieri, R. Falcone, S. Lee, R. Pahl, J. Rudati, P. Fuoss, A. Nelson, P. Krejcik, D. Siddons, P. Lorazo, J. Hastings, Phys. Rev. Lett. **100**, 135502 (2008)
28. M. Ligges, I. Rajkovic, P. Zhou, O. Posth, C. Hassel, G. Dumpich, D. von der Linde, Appl. Phys. Lett. **94**, 101910 (2009)
29. S. Preuss, A. Demchuk, M. Stuke, Appl. Phys. A **61**, 33 (1995)
30. P.P. Pronko, S.K. Dutta, J. Squier, J.V. Rudd, D. Du, G. Mourou, Opt. Commun. **114**, 106 (1995)
31. C. Momma, B.N. Chichkov, S. Nolte, F. von Alvensleben, A. Tünnermann, H. Welling, Opt. Commun. **129**, 134 (1996)
32. B.C. Stuart, M.D. Feit, S. Herman, A.M. Rubenchik, B.W. Shore, M.D. Perry, J. Opt. Soc. Am. B **13**, 459 (1996)
33. W. Kautek, J. Krüger, M. Lenzner, S. Sartania, C. Spielmann, F. Krausz, Appl. Phys. Lett. **69**, 3146 (1996)
34. B. Chichkov, C. Momma, S. Nolte, F. von Alvensleben, A. Tünnermann, Appl. Phys. A **63**, 109 (1996)
35. S. Nolte, C. Momma, H. Jacobs, A. Tünnermann, B.N. Chichkov, B. Wellegehausen, H. Welling, J. Opt. Soc. Am. B **14**, 2716 (1997)
36. F. Korte, S. Nolte, B.N. Chichkov, T. Bauer, G. Kamlage, T.Wagner, C. Fallnich, H. Welling, Appl. Phys. A **69**, S7 (1999)
37. N. Bärsch, K. Körber, A. Ostendorf, K.H. Tönshoff, Appl. Phys. A **77**, 237 (2003)
38. G. Kamlage, T. Bauer, A. Ostendorf, B.N. Chichkov, Appl. Phys. A **77**, 307 (2003)
39. S. Ameer-Beg, W. Perrie, S. Rathbone, J. Wright, W. Weaver, H. Champoux, Appl. Surf. Sci. **127–129**, 875 (1998)
40. R. Haight, D. Hayden, P. Longo, J. Vac. Sci. Technol. B **17**, 3137 (1999)
41. K. Ozono, M. Obara, A. Usui, H. Sunakawa, Opt. Commun. **189**, 103 (2001)

42. N.H. Rizvi, Riken Rev. **50**, 107 (2003)
43. R. LeHarzic, N. Huot, E. Audouard, C. Jonin, P. Laporte, placeS. Valette, A. Fraczkiewicz, R. Fortunier, Appl. Phys. Lett. **80**, 3886 (2002)
44. F. Garrelie, A.S. Loir, C. Donnet, F. Rogemont, R. LeHarzic, M. Belin, E. Audouard, F. Laporte, Surf. Coat. Technol. **163–164**, 306 (2003)
45. R. Eason, *Pulsed Laser Deposition of Thin Films* (Wiley, 2007)
46. F. Garrelie, C. Donnet, A.S. Loir, N. Benchikh, SPIE Proceedings **6261**, 62610L (2006)
47. K. Kawamura, N. Sarukura, M. Hirano, N. Ito and H. Hosono, Appl. Phys. Lett. **79**, 1228–1130 (2001)
48. J. Bonse, P. Rudolph, J. Krüger, S. Baudach, W. Kautek, Appl. Surf. Sci. **154–155**, 659 (2000)
49. G. Dumitru, V. Romano, Y. Gerbig, H.P. Weber, H. Haefke, Appl. Phys. A **80**, 283 (2005)
50. A. Marcinkevicius, S. Juodkazis, M. Watanabe, M. Miwa, S. Matsuo, H. Misawa, J. Nishii, Opt. Lett. **26**, 277 (2001)
51. K. Minoshima, A.M. Kowalevicz, I. Hartl, E.P. Ippen, J.G. Fujimoto, Opt. Lett. **26**, 1516 (2001)
52. M. Masuda, K. Sugioka, Y. Cheng, T. Hongo, K. Shihoyama, H. Takai, placeI. Miyamoto, K. Midorikawa, Appl. Phys. A **78**, 1029 (2004)
53. K. Miura, Jianrong Qiu, S. Fujiwara, S. Sakaguchi, K. Hirao, Appl. Phys. Lett. **80**, 2263 (2002)
54. Ken-ichi Kawamura, Masahiro Hirano, Toshio Kamiya, Hideo Hosono, Appl. Phys. Lett. **81**, 1137 (2002)
55. F. Korte, J. Serbin, J. Koch, A. Egbert, C. Fallnich, A. Ostendorf, B.N. Chichkov, Appl. Phys. A **77**, 229 (2003)
56. K. Sugioka, M. Masuda, T. Hongo, Y. Cheng, K. Shihoyama, K. Midorikawa, Appl. Phys. A **79**, 815 (2004)
57. K.M. Davis, K. Miura, placeN. Sugimoto, K. Hirao, Opt. Lett. **21**, 1729 (1996)
58. S. Nolte, M. Will, J. Burghoff, A. Tuennermann, Appl. Phys. A **77**, 109 (2003)
59. R. Osellame,G. Della Valle, N. Chiodo, S. Taccheo, P. Laporta,O. Svelto, G. Cerullo, Appl. Phys. A **93**, 17 (2008)
60. L. Shah, A.Y. Arai, S.M. Eaton, P.R. Herman, Opt. Express **13**, 1999 (2005)
61. L. Li, J.T. Fourkas, Mater. Today **10**, 30 (2007)
62. J. Serbin, A. Egbert, A. Ostendorf, B.N. Chichkov, R. Houbertz, G. Domann, J. Schulz, C. Cronauer, L. Fröhlich, M. Popall, Opt. Lett. **28**, 301 (2003)
63. Y. Cheng, K. Sugioka, K. Midorikawa, M. Masuda, K. Toyoda, M. Kawachi, K. Shihoyama, Opt. Lett. **28**, 1144 (2003)
64. Fraunhofer-Institut für Silicatforschung, Wuerzburg, Germany
65. J.-M Shieh, Z.-H. Chen, B.-T. Dai, Y.-C. Wang, A. Zaitsev, C.-L. Pan, Appl. Phys. Lett. **85**, 1232 (2004)
66. J. Jia, M. Li, C.V. Thompson, Appl. Phys. Lett. **84**, 3205 (2004)
67. Y. Hosokawa, H. Takabayashi, S. Miura, C. Shukunami, Y. Hiraki, H. Masuhara, Appl. Phys. A **79**, 795 (2004)
68. W. Supatto, D. Débarre, B. Moulia, E. Brouzés, J.-L. Martin, E. Farge, E. Beaurepaire, PNAS **102**, 1047 (2005)
69. A. Vogel, J. Noack, G. Hüttmann, G. Paltauf, Appl. Phys. B **81**, 1015 (2005)
70. A. Heisterkamp, I.Z. Maxwell, E. Mazur, J.M. Underwood, J.A. Nickerson, S. Kumar, D.E. Ingber, Opt. Express **13**, 3690 (2005)
71. K. König, O. Krauss, I. Riemann, Opt. Express **10**, 171 (2002)
72. I. Zergioti, A. Karaiskou, D.G. Papazoglou, C. Fotakis, M. Kapsetaki, D. Kafetzopoulos, Appl. Phys. Lett. **86**, 163902 (2005)
73. K. Ozono, M. Obara, Appl. Phys. A **77**, 303 (2003)
74. J. Serbin,T. Bauer, C. Fallnich, A. Kasenbacher, W.H. Arnold, Appl. Surf. Sci. **197–198**, 737 (2002)
75. S. Eliezer, N. Eliaz, E. Grossman, D. Fisher, I. Gouzman, Z. Henis, S. Pecker, Y. Horovitz, M. Fraenkel, S. Maman, Y. Lereah, Phys. Rev. B **69**, 144119 (2004)
76. Andrei V. Kabashin, Michel Meunier, Christopher Kingston, and John H.T. Luong, J. Phys. Chem. B **107**, 4527 (2003)

77. A.V. Kabashin, M. Meunier, J. Appl. Phys. **94**, 7941 (2003)
78. S. Amoruso, R. Bruzzese, N. Spinelli, R. Velotta, M. Vitiello X. Wang, G. Ausanio, V. Iannotti, L. Lanotte, Appl. Phys. Lett. **84**, 4502 (2004)
79. R. Wagner, J. Gottmann, A. Horn, E.W. Kreutz, Appl. Surf. Sci. **252**, 8576 (2006)
80. N. Sanner, N. Huot, E. Audouard, C. Larat, J.-P. Huignard, Opt. Las. Eng. **45**, 737 (2007)
81. M. Zamfirescu, M. Ulmeanu, F. Jipa, O. Cretu, A. Moldovan, G. Epurescu, M. Dinescu, R. Dabu, J. Laser Micro/Nanoeng. **4**, 7, 2009
82. G.R.B.E. Römer, A.J.Huis in't Veld, J. Meijer, M.N.V. Groenendijk, CIRP Ann. Manufact. Technol. **58**, 201 (2009)